Single Image Atmospheric Veil Removal Using New Priors

Alexandra Duminil, Jean-Philippe Tarel, Roland Brémond

2021 IEEE International Conference on Image Processing (ICIP) | 978-1-6654-4115-5/21/$31.00 ©2021 IEEE | DOI: 10.1109/ICIP42928.2021.9506244

SINGLE IMAGE ATMOSPHERIC VEIL REMOVAL USING NEW PRIORS

Alexandra Duminil *Jean-Philippe Tarel* *Roland Brémond*

COSYS-PICS-L
Univ. Gustave Eiffel
F-77454 Marne-la-Vallée, France
Email: alexandra.duminil@univ-eiffel.fr

ABSTRACT

From an analysis of the priors used in previous algorithms for single image defogging, a new prior is proposed to obtain a better atmospheric veil removal. The Naka-Rushton function is used to modulate the atmospheric veil according to empirical observations on synthetic foggy images. The parameters of this function are set from features of the input image. The algorithm is able to take into account different kinds of airborne particles and different illumination conditions. The proposed method is extended to nighttime and underwater images by computing the atmospheric veil on each color channel. Qualitative and quantitative evaluations show the benefit of the proposed algorithm.

Index Terms— Visibility Restoration, Single Image Defogging, Bad Weather conditions, Atmospheric Veil, Naka-Rushton.

1. INTRODUCTION

Visibility restoration of outdoor images is a well-known problem in both computer vision applications and digital photography, particularly in adverse weather conditions such as fog, haze, rain and snow. Such weather conditions cause visual artifacts in the images such as loss of contrast and color shift, which contributes to reduce scene visibility. The lack of visibility can be detrimental for the performance of automated systems based on image segmentation [1] and object detection [2], and thus requires visibility restoration as a pre-processing [3] step. With fog or haze, contrast reduction is caused by the atmospheric veil. With rain or snow, it is caused by the occlusion of the distant background by raindrops or snowflakes.

This paper proposes two contributions: the first one is the use of the Naka-Rushton function in the inference of the atmospheric veil. The parameters of this function are estimated from the characteristics of the input foggy image. The second contribution is the restoration of images with other kinds of airborne particles and heterogeneous illumination, such as nighttime and underwater images, by processing each color channel separately. Some of these contributions have been proposed in [4]. The paper is organized as follows: Section 2 introduces the problem and related works. Section 3 presents the proposed visibility restoration method and Section 4 shows experimental results with qualitative and quantitative evaluations and comparisons.

Thanks to FEREC project OCAPI for funding.

2. RELATED WORKS

2.1. Fog Visual Effect

Koschmieder's law is a straightforward optical model which describes the visual effects of the scattering of daylight by the particles fog is made of [3]. When fog and illumination are homogeneous along a light path going through x, the model is:

$$I(x) = J(x)t(x) + A(1 - t(x)) \quad (1)$$

where $I(x)$ is the foggy image, $J(x)$ the fog-free image, A the sky intensity, $x = (u, v)$ denotes the pixel coordinates. The transmittance $t(x) = e^{-kd(x)}$ describes the percentage of light which is not scattered, where k is the extinction coefficient, which is related to the density of fog, and $d(x)$ is the distance between the camera and the objects in the scene. The atmospheric veil is the last term in Eq. (1).

2.2. Daytime Image Defogging

Single image defogging algorithms can be divided into two categories. Image enhancement algorithms use ad-hoc techniques to improve the image contrast such as histogram equalisation and retinex, but they do not account for scene depth. Visibility restoration, on which we focus, are model-based and use Koschmieder's law. Since depth is unknown, the problem is an ill-posed inverse problem that requires priors to be solved. Priors may be introduced as constrains or using a learning dataset.

In [3], geometric priors are introduced. He et al. [5, 6] introduced the Dark Channel Prior (DCP) as a method dedicated to color images. The idea is that fog-free outdoor images contain pixels with very low intensity in at least one of

the three color channels in any pixel neighborhood. Variants and extensions were proposed such as [7, 8, 9].

In the last five years, learning-based methods have been proposed for defogging, usually based on Convolutional Neural Networks (CNN) with supervised training [10, 11, 12, 13, 14]. Fog is a rather unpredictable phenomenon, so building a large and representative training dataset with pairs of images with and without fog is very difficult. This leads to generalization problems. More recently, GAN networks have been used [15], with partially supervised training databases, but the learning control is complicated. Fog removal being a preprocessing, fast and computationally inexpensive algorithms are usually required. We thus focus here on algorithms with very few parameters to be learned.

2.3. Hidden Priors in the DCP Method

In DCP [5, 6], a widely used parameter called ω was clearly introduced in the transmission map computation:

$$t(x) = 1 - \omega \min_{c} \left(\min_{y \in \Omega(x)} \left(\frac{I^c(y)}{A^c} \right) \right) \qquad (2)$$

were $\Omega(x)$ is the local patch centered on x, c the color channel, A the sky intensity, and I the image intensity. This parameter was introduced to mitigate over-restoration, and it is usually set to $\omega = 0.95$. According to [5], it maintains a small amount of haze in the distance, producing more natural results.

This parameter is actually a prior and needs to be explicited. First, let us propose a different interpretation of ω. The term $\min_c(\min_{y \in \Omega(x)}(I^c(y)))$ in the transmittance Eq. (2) is a first estimation of the atmospheric veil, based on the white fog and the locally smooth fog priors. The result is a mixture between the actual atmospheric veil and the luminance of objects in the scene. Let us name it the "pre-veil". The percentage of the pre-veil which corresponds to the real atmospheric veil is unknown, it is assumed to be constant and equal to ω across the image. Therefore, ω can be explicitly described as a prior parameter: it is the assumed constant percentage of atmospheric veil in the pre-veil map.

We test the validity of this prior in the next section.

3. SINGLE IMAGE ATMOSPHERIC VEIL REMOVAL

3.1. Is the use of ω a valid prior?

The usual way to compute the atmospheric veil from the pre-veil is to apply the parameter ω. To test the validity of this prior, we have to look at the link between the intensities in the true veil and in the pre-veil images. This can only be achieved with a synthetic image database, so we used the generator of the FRIDA dataset [8]. In this synthetic images, the veil is computed using Koschmieder's law from the scene depth map. Thus, the atmospheric veil map can be computed for each generated foggy image. Fig. 1 (a) shows the histogram of fifty foggy images, with the pre-veil image intensities on the horizontal axis and the intensities of the ground truth atmospheric veil on the vertical axis.

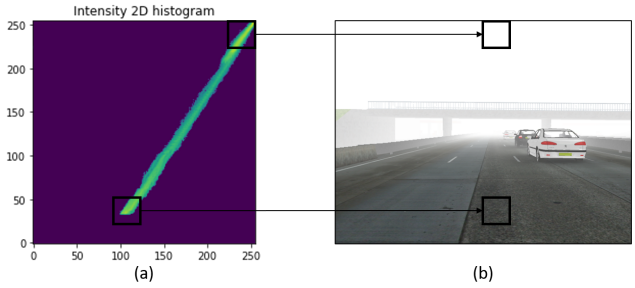

Fig. 1: Foggy pixels and veil pixels intensities: (a) histogram showing the link between pre-veil and veil pixel intensities (Mean of fifty images from the FRIDA dataset [8]), (b) input foggy image.

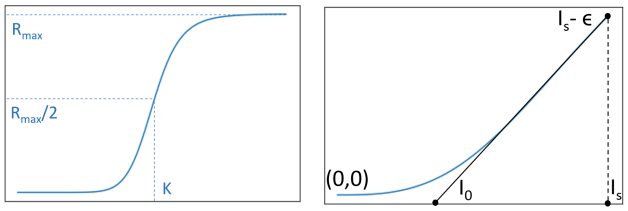

Fig. 2: Left: the Naka-Rushton function with parameters R_{max}, K and n. Right: the modulation function, shaped like the lefthand side of the Naka-Rushton function, showing parameters I_s, I_0 and ϵ.

Fig. 1(a) shows that the link between foggy pixel intensities and associated veil intensities is roughly affine. The intensity of the atmospheric veil is high in the sky region, and it is low in the ground region which is closer to the camera. Since the variation is affine, it can not be modeled well with a constant parameter such as ω. A function would be more relevant.

3.2. Modulation function as a prior

To avoid over-restoration at the bottom of the image but to ensure that the restoration is maximum at the top of the image, a modulation function f is necessary to compute the atmospheric veil from the pre-veil. This function should be smooth to avoid visual artefacts in the restored image.

From Fig. 1(a), the following constraints are proposed to chose a function f which will appropriately modulate the pre-veil:

1. The function f should be roughly linear on a large range of intensities. This range is denoted $[I_0, I_s]$. We introduce here the slope a of f at I_s, i.e. $f'(I_s) = a$.

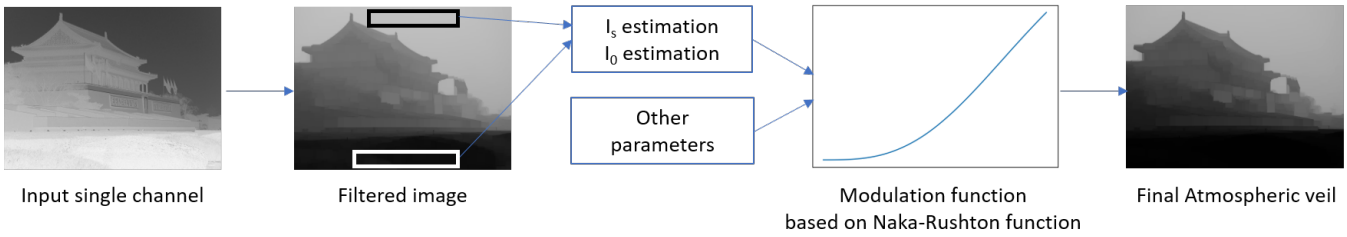

Fig. 3: Atmospheric veil estimation from the morphologically filtered pre-veil using Naka-Rushton as a modulation function.

2. The function is close to zero on the intensity range $[0, I_0]$, i.e. for the intensities of pixels looking at objects which are close to the camera where fog cannot be seen.

3. The function and the restored image must not be negative.

4. I_s is the intensity of the clearest (sky) region. To avoid too dark values in the corresponding areas, $f(I_s)$ should be a little lower than I_s. We thus introduce a parameter ϵ such that $f(I_s) = I_s - \epsilon$ in order to preserve the sky. ϵ is smoothly estimated as a function of I_s.

Among the different functions we tested, the Naka-Rushton [16] function was the easier to tune. This function was first introduced to describe the biological response of a neuron, and was further used in computer graphics for the tone-mapping problem. It is defined as:

$$R(x) = R_{max}\frac{x^n}{x^n + K^n} \tag{3}$$

where R_{max} is its upper-bound, K is the horizontal position of the inflection point and n is related to the slope at the inflection point (see Fig. 2). The shape of the first part of the curve in Fig. 2 (left) fits our needs, as shown in Fig. 2 (right). The inflexion point with coordinates $(K, \frac{R_{max}}{2})$ should correspond to the modulation function f at I_s.

3.3. Naka-Rushton function parameters

R_{max}, K and n are the parameters of the Naka-Rushton function, whereas the parameters of the modulation function f are I_0, I_s, and ϵ. In the previous section, K was set to I_s. Following constraint 4. in Sec. 3.2, $f(I_s)$ is set to $I_s - \epsilon$. Thus, $R_{max} = 2(I_s - \epsilon)$. The slope at I_s is set to a. This slope in the Naka-Rushton function being $\frac{nR_{max}}{4K}$ (obtained by deriving the Naka-Rushton function), we have $n = \frac{2I_s a}{I_s - \epsilon}$. It follows that $a = \frac{I_s - \epsilon}{I_s - I_0}$. The parameter a was calculated as the slope between the points of coordinates $(I_0, 0)$ and $(I_s, I_s - \epsilon)$ (see the right image in Fig. 2).

Finally, the proposed modulation function f is:

$$f(x) = f_0\frac{x^n}{x^n + k^n} \tag{4}$$

where $f_0 = 2(I_s - \epsilon)$, $k = I_s$, $n = \frac{2I_s a}{I_s - \epsilon}$ and $a = \frac{I_s - \epsilon}{I_s - I_0}$. This modulation function has only three parameters: I_0, I_s, and ϵ. The last one must be set to a small value, the other two can be computed from the input image.

In Fig. 1(b), I_s is the intensity of the sky and I_0 is the intensity of the ground close to the camera. We have investigated how I_0 and I_s can be best estimated. Taking the maximum of the image intensities for I_s and the minimum for I_0 is too sensitive to noise. Therefore, I_0 and I_s are computed by taking, respectively, the minimum and the maximum of the input foggy image after using a morphological closing followed by a morphological opening. The veil processing is shown in Fig. 3.

3.4. Beyond the White Fog Prior

In order to better handle colored atmospheric veil, we propose a simple method: processing each color channel separately with our algorithm. This is possible only because the proposed atmospheric veil removal method is able to process gray-level images thanks to the use of the modulation function prior. By processing each color channel separately, I_s is estimated on each channel and thus the color of the veil is inferred.

4. EXPERIMENTAL RESULTS

The proposed algorithm is compared with six state-of-the-art algorithms included three prior-based methods and three learning-based methods: DCP [6], NBPC [7], Zhu et al [9], AOD-Net [13], Dehaze-Net [10] and GCA-Net [14]. We selected algorithms whose codes were publicly available. For each algorithm, we optimized all the input parameters, except the ω parameter in the DCP which is set to 0.95 in the original paper. We tested different values of each parameter on four datasets using SSIM [17] and PSNR as comparison criteria. We first present a quantitative comparison on synthetic images from the public FRIDA dataset [8], the Synthetic Objective Testing Set (SOTS) from the RESIDE dataset [18], NTIRE20 dataset and O-HAZE dataset [19]. Then we present a qualitative comparison on real world images.

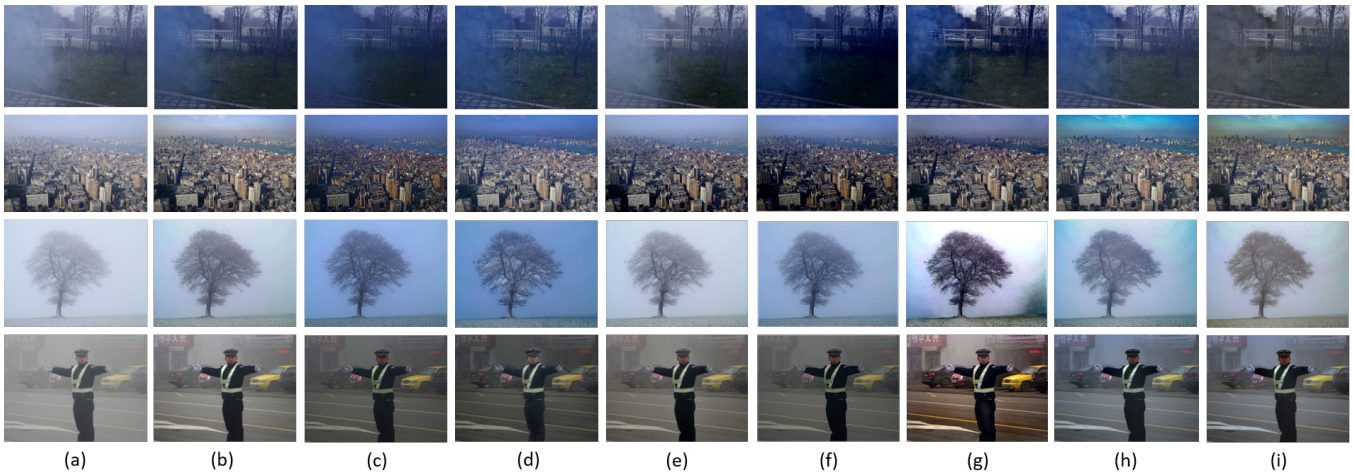

Fig. 4: Comparison of fog removal results on real world image: (a) input foggy images, (b) DCP, (c) NBPC, (d) Zhu et al., (e) Dehaze Net, (f) AOD Net (g) GCA Net, (h) W and (i) C.

4.1. Quantitative Evaluation

	SSIM/PSNR			
Methods	FRIDA	SOTS	NTIRE20	O-HAZE
DCP	0.70/12.26	0.89/18.91	0.44/12.77	**0.66**/16.95
NBPC	0.75/11.59	0.89/18.07	0.41/12.24	0.61/15.85
Zhu et al.	0.72/12.15	0.88/16.06	0.45/11.98	**0.66**/16.58
AOD-Net	0.73/10.73	0.85/19.39	0.41/11.98	0.54/15.04
Dehaze-Net	0.65/10.87	**0.90/23.41**	0.44/12.33	0.60/15.41
GCA-Net	0.70/**12.79**	**0.91/22.68**	0.47/12.82	0.61/16.43
W	**0.81/12.62**	0.85/17.23	**0.51/13.16**	0.65/17.02
C	**0.81**/12.27	0.82/16.77	**0.51/13.90**	**0.67/18.32**

Table 1: Comparison of the SSIM and PSNR indexes on four datasets: fifty images from the FRIDA, SOTS datasets, forty-five images from the NTIRE20 and O-HAZE datasets. W corresponds to our main algorithm assuming white fog, and C is the color version (see Sec. 3.4).

Results are shown in Tab. 1 and illustrate that all methods are competitive, but our methods outperform the others with both criteria on FRIDA, Ntire20 and O-HAZE datasets. The results on the SOTS dataset show that the proposed algorithm is less efficient on images where the veil is spatially close to uniform.

4.2. Qualitative Evaluation

Real world images from previous works on fog removal have been used for a qualitative comparison. On Fig. 4, DCP, NBPC and Zhu et al. algorithms remove the fog with good results. However, DCP images are bright and contrasted, while NBPC and Zhu et al.'s results are darker and more faded. The learning-based method AOD-Net provides dark and faded results but with less halos. It appears in the tree and buildings images that Dehaze-Net method retains far away haze. It better works on images with colored sky regions by avoiding artefacts and blue-shift distortions unlike most of other algorithms. GCA-Net produces artefacts in sky region of the tree image but provides good and colored results in others particularly in the last line image.

The first version of our algorithm (Fig. 4 (h)) provides bright results and removes the haze over the entire images. The color version (Fig. 4 (i)) allows reducing blue color distortions.

5. CONCLUSION

We have reinterpreted the DCP method in terms of three priors. We propose to improve the third prior, associated to ω, with a smooth modulation function as a prior to estimate the atmospheric veil from the pre-veil. The input parameters of this function are automatically estimated according to the input image pixel intensities in light (sky) and dark (ground) regions. The proposed method provides good results on both synthetic and real world images for objects at all distances.

To extend the proposed algorithm to rain, smoke, dust and other colored airborne particles, we process each color channel separately, in order to remove colored components. This allows to apply the algorithm to nighttime images as well as underwater images. The proposed algorithm should be carefully evaluated on these diverse conditions. This is not easy with real world images, as ground truth are very difficult to build.

A few color artifacts have been observed when restoring sky regions of objects at large distances. In the future, we will thus investigate these limits, trying to avoid artifacts and preserve a better color consistency.

6. REFERENCES

[1] Maxime Tremblay, Shirsendu Halder, Raoul De Charette, and Jean-François Lalonde, "Rain rendering for evaluating and improving robustness to bad weather," vol. accepted, 2020.

[2] S. C. Huang, T. H. Le, and D. W. Jaw, "Dsnet: Joint semantic learning for object detection in inclement weather conditions," *IEEE Transactions on Pattern Analysis and Machine Intelligence*, pp. 1–1, 2020.

[3] Nicolas Hautière, Jean-Philippe Tarel, and Didier Aubert, "Towards fog-free in-vehicle vision systems through contrast restoration," in *IEEE Conference on Computer Vision and Pattern Recognition (CVPR'07)*, Minneapolis, Minnesota, USA, 2007, pp. 1–8, http://perso.lcpc.fr/tarel.jean-philippe/publis/cvpr07.html.

[4] Alexandra Duminil, Jean-Philippe Tarel, and Brémond Roland, "Single image atmospheric veil removal using new priors for better genericity," *To appear in Atmosphere*, 2021.

[5] Kaiming He, Jian Sun, and Xiaoou Tang, "Single image haze removal using dark channel prior," in *2009 IEEE Conference on Computer Vision and Pattern Recognition*. IEEE, 2009, pp. 1956–1963.

[6] Kaiming He, Jian Sun, and Xiaoou Tang, "Single Image Haze Removal Using Dark Channel Prior," *IEEE Transactions on Pattern Analysis and Machine Intelligence*, vol. 33, no. 12, pp. 2341–2353, Dec. 2011.

[7] Jean-Philippe Tarel and Nicolas Hautiere, "Fast visibility restoration from a single color or gray level image," in *2009 IEEE 12th International Conference on Computer Vision*, Kyoto, Sept. 2009, pp. 2201–2208, IEEE.

[8] J-P Tarel, N. Hautiere, L. Caraffa, A. Cord, H. Halmaoui, and D. Gruyer, "Vision Enhancement in Homogeneous and Heterogeneous Fog," *IEEE Intelligent Transportation Systems Magazine*, vol. 4, no. 2, pp. 6–20, 2012.

[9] Mingzhu Zhu, Bingwei He, and Qiang Wu, "Single Image Dehazing Based on Dark Channel Prior and Energy Minimization," *IEEE Signal Processing Letters*, vol. 25, no. 2, pp. 174–178, Feb. 2018.

[10] Bolun Cai, Xiangmin Xu, Kui Jia, Chunmei Qing, and Dacheng Tao, "DehazeNet: An End-to-End System for Single Image Haze Removal," *IEEE Transactions on Image Processing*, vol. 25, no. 11, pp. 5187–5198, Nov. 2016.

[11] Wenqi Ren, Si Liu, Hua Zhang, Jinshan Pan, Xiaochun Cao, and Ming-Hsuan Yang, "Single Image Dehazing via Multi-scale Convolutional Neural Networks," in *Computer Vision – ECCV 2016*, Bastian Leibe, Jiri Matas, Nicu Sebe, and Max Welling, Eds., Cham, 2016, Lecture Notes in Computer Science, pp. 154–169, Springer International Publishing.

[12] Tim Meinhardt, Michael Moeller, Caner Hazirbas, and Daniel Cremers, "Learning Proximal Operators: Using Denoising Networks for Regularizing Inverse Imaging Problems," in *2017 IEEE International Conference on Computer Vision (ICCV)*, Venice, Oct. 2017, pp. 1799–1808, IEEE.

[13] Boyi Li, Xiulian Peng, Zhangyang Wang, Jizheng Xu, and Dan Feng, "An All-in-One Network for Dehazing and Beyond," *arXiv:1707.06543 [cs]*, July 2017.

[14] D. Chen, M. He, Q. Fan, J. Liao, L. Zhang, D. Hou, L. Yuan, and G. Hua, "Gated Context Aggregation Network for Image Dehazing and Deraining," in *2019 IEEE Winter Conference on Applications of Computer Vision (WACV)*, Jan. 2019, pp. 1375–1383, ISSN: 1550-5790.

[15] Deniz Engin, Anil Genc, and Hazim Kemal Ekenel, "Cycle-Dehaze: Enhanced CycleGAN for Single Image Dehazing," in *2018 IEEE/CVF Conference on Computer Vision and Pattern Recognition Workshops (CVPRW)*, Salt Lake City, UT, USA, June 2018, pp. 938–9388, IEEE.

[16] K. I. Naka and W. a. H. Rushton, "S-potentials from colour units in the retina of fish (Cyprinidae)," *The Journal of Physiology*, vol. 185, no. 3, 1966.

[17] Z. Wang, A.C. Bovik, H.R. Sheikh, and E.P. Simoncelli, "Image Quality Assessment: From Error Visibility to Structural Similarity," *IEEE Transactions on Image Processing*, vol. 13, no. 4, pp. 600–612, Apr. 2004.

[18] B. Li, W. Ren, D. Fu, D. Tao, D. Feng, W. Zeng, and Z. Wang, "Benchmarking Single-Image Dehazing and Beyond," *IEEE Transactions on Image Processing*, vol. 28, no. 1, pp. 492–505, Jan. 2019, Conference Name: IEEE Transactions on Image Processing.

[19] Codruta O. Ancuti, Cosmin Ancuti, Radu Timofte, and Christophe De Vleeschouwer, "O-HAZE: A Dehazing Benchmark With Real Hazy and Haze-Free Outdoor Images," 2018, pp. 754–762.